THE UNIVERSITY *of* EDINBURGH

Edinburgh Research Explorer

The gas-phase structure of the decasilsesquioxane $Si_{10}O_{15}H_{10}$

Link:
Link to publication record in Edinburgh Research Explorer

Document Version:
Publisher's PDF, also known as Version of record

Published In:
Dalton Transactions

OPEN ACCESS

The gas-phase structure of the decasilsesquioxane $Si_{10}O_{15}H_{10}$†

Derek A. Wann,[a] Franck Rataboul,[b] Anthony M. Reilly,[a] Heather E. Robertson,[a] Paul D. Lickiss[b] and David W. H. Rankin[a]

The equilibrium molecular structure of the decasilsesquioxane, $Si_{10}O_{15}H_{10}$, in the gas phase has been determined by gas electron diffraction. Molecular dynamics calculations were used to give amplitudes of vibration and differences between interatomic distances in the equilibrium structure and the vibrationally averaged distances that are given directly by the diffraction data. The molecules have D_{5h} symmetry, and do not show the distortions that are apparent in the crystalline phase. The ten-membered silicon-oxygen rings are found to be particularly flexible in the gas phase, a phenomenon that was also seen in crystal structures. The Si–O bond lengths in the ten-membered rings are 161.6(2) pm long and in the eight-membered rings they are 162.2(3) pm, with Si–O–Si angles of 155.0(5) and 153.9(7)°, respectively.

Introduction

Polyhedral oligosilsesquioxanes, particularly those of the general formula $Si_8O_{12}R_8$, have become of significant interest because of their useful properties and their potential as precursors to many novel nanocomposites and polymers.[1,2] Much less widely studied, but of increasing importance, are the related decasilsesquioxanes, $Si_{10}O_{15}R_{10}$, the simplest of which is the decahydridosilsesquioxane, $Si_{10}O_{15}H_{10}$. This silsesquioxane, originally reported in 1970,[3] is formed in low yield, along with other higher silsesquioxanes, as a by-product of the hydrolysis of $HSiCl_3$ during the synthesis $Si_8O_{12}H_8$.[4–6]

The solid-state structure of $Si_{10}O_{15}H_{10}$ has been determined by single-crystal X-ray diffraction at 180 and at 295 K.[7] The structure at 180 K has average Si–O distances of 161.2(2) and 160.1(5) pm, Si–O–Si angles of 149.5(17) and 154.7(31)°, and O–Si–O angles of 110.0(2) and 109.5(2)°, in each case for the eight- and ten-membered rings, respectively. The distributions of individual values within the Si–O and O–Si–O values show small deviations from those for a structure of ideal D_{5h} symmetry but the Si–O–Si angle ranges are much larger [147.43(13) to 150.64(12) and 151.51(14) to 159.53(15)° within the eight- and ten-membered rings, respectively]. This wide range of angles for symmetrically substituted polyhedral oligosilsesquioxanes in the solid state has been noted previously for the related $Si_8O_{12}R_8$ compounds.[1]

Geometry optimisations of isolated molecules of $Si_{10}O_{15}H_{10}$ have previously been reported and, as would be expected, do not show the range of angles found in the solid-state structure determinations.[8–11] Calculations have also been carried out on the structures and properties of endohedral complexes of $Si_{10}O_{15}H_{10}$ cages with various atoms and ions, showing that there is space within the polyhedron to accommodate a range of species. Endohedral complexes with, for example, Li^+, Na^+, F^- and Br^- are found to be favoured and encapsulation of the alkali metal cations leads to cage shrinkage.[8] Calculations on the viability of inserting N_2 or O_2 through the Si_5O_5 face of the polyhedron have also been carried out.[9]

The vibrational spectra of $Si_{10}O_{15}H_{10}$ have been studied in detail for solutions,[12,13] the solid phase[12,14,15] and when deposited onto a surface.[13,16] Binding energies for $Si_{10}O_{15}H_{10}$ on surfaces have also been determined by photoemission spectroscopy.[16,17] The potential of $Si_{10}O_{15}H_{10}$ as a CVD precursor to high-quality SiO_2 films has been demonstrated,[18] as has its use as a component in a photosensitive resist film.[19]

The work presented in the current study provides the first experimental determination of the structure of a decasilsesquioxane in the gas phase, giving structural parameters for the polyhedral compound that are not perturbed by solid-state packing effects and which may be compared to calculated structures. This also allows comparison of the data for $Si_{10}O_{15}H_{10}$ with D_{5h} symmetry with the gas-phase data for the related $Si_8O_{12}H_8$ of O_h symmetry.[20]

[a]School of Chemistry, University of Edinburgh, West Mains Road, Edinburgh, UK EH9 3JJ. E-mail: d.w.h.rankin@ed.ac.uk
[b]Department of Chemistry, Imperial College London, South Kensington, London, UK SW7 2AZ

† Electronic supplementary information (ESI) available: Tables of experimental parameters for the GED analysis of $Si_{10}O_{15}H_{10}$ (Table S1), calculated coordinates at the MP2/6-311++(3df,3pd) level (Table S2), refined and calculated RMS amplitudes of vibration (u), associated r_a distances and corresponding perpendicular correction values (k) (Table S3), GED-determined atomic coordinates (Table S4) and least-squares correlation matrix (Table S5) for the refinement of $Si_{10}O_{15}H_{10}$. Molecular-intensity scattering and difference curves for $Si_{10}O_{15}H_{10}$ (Figure S1) are given as well as diagrammatic representations of the eigenvectors corresponding to the two lowest frequency vibrations as calculated at the RHF/6-31G(d) level (Figures S2 and S3). See DOI: 10.1039/b909136j

Experimental

Computational studies

Series of calculations were performed using the Gaussian 03 suite of programs,[21] to assess how the computed molecular geometry of $Si_{10}O_{15}H_{10}$ is affected by different levels of theory and basis sets. The calculations were carried out using the resources of the EPSRC National Service for Computational Chemistry Software.[22] Calculations were initially performed using the spin-restricted Hartree–Fock (RHF) method with the 3-21G(d) basis

set[23] before further calculations were carried out using larger basis sets, namely 6-31G(d),[24] 6-311+G(d),[25] 6-311++G(d,p) and 6-311++G(3df,3pd). Electron correlation was included using second-order Møller–Plesset perturbation theory (MP2)[26] and density functional theory (DFT) calculations were carried out using the hybrid functional B3LYP.[27] Further B3LYP calculations were performed using the aug-cc-pVDZ basis set.[28]

As electron-diffraction experiments yield time-averaged structures, in which the effects of vibrations may alter interatomic distances, it is common to compute corrections to apply to the distances. This allows more accurate comparison of theoretical and experimental structures to be made. Here, the molecular dynamics method of obtaining distance corrections and starting values of amplitudes of vibrations has been used. This method is discussed in greater detail elsewhere[29] and only details of the calculations pertinent to this work are given.

Plane-wave density functional theory (PW-DFT) calculations were performed with the Car–Parrinello molecular dynamics (CPMD) code[30] using the resources of the Edinburgh Parallel Computing Centre. To model an isolated molecule using a periodic code, such as CPMD, a single molecule is simulated in a supercell large enough to minimise any interactions between the molecule and its periodic images. In the present study the Tuckerman–Poisson solver[31] was used to decouple the electrostatic interactions, allowing a supercell of 1.5 nm to be used. The PBE exchange–correlation functional[32] was used and the core-valence interaction was represented with Troullier–Martins norm-conserving pseudopotentials.[33] A plane-wave cut-off energy of 1600 eV was adopted for the calculations.

The equilibrium geometry of $Si_{10}O_{15}H_{10}$ was optimised, starting from the geometry calculated at the MP2/6-311++G(3df,3pd) level, until the energy change per atom and maximum atomic force fell below 1×10^{-8} eV and 1 meV, respectively. This structure was then used to determine the correction terms by carrying out a molecular dynamics simulation. The simulation was performed in the canonical (NVT) ensemble using a chain of three Nosé–Hoover thermostats[34,35] to regulate the simulation temperature at 423 K, approximately the temperature of the experiment. A thermostat frequency of 2200 cm⁻¹ was adopted. The simulation was run using the Car–Parrinello formulism[36] with an electronic time step of 75.57 as. The geometry was sampled every 15 steps and data were collected for a total of 22 ps.

As discussed in reference 29, the MD simulations do not yield accurate amplitudes of vibration for pairs of atoms with stretching modes involving hydrogen because of quantum mechanical tunnelling. The dynamics of the nuclei in an MD simulation are treated in a classical fashion even with the quantum-mechanically derived forces. With the hydrogen atom this leads to significant underestimation of the Si–H stretching motion. For this reason the Si–H amplitude was substituted with a standard starting value of 7.5 pm. The motion of heavier atoms and non-bonded pairs is sufficiently approximated by the classical dynamics.

Gas electron diffraction

Data were collected for $Si_{10}O_{15}H_{10}$ using the Edinburgh gas-phase electron diffraction (GED) apparatus[37] with an accelerating voltage of 40 kV (equivalent to an electron wavelength of approximately 6.0 pm). The experiments were performed at two different nozzle-to-film distances to maximise the range of scattering data available. The scattering intensities were recorded on Kodak Electron Image films; nozzle-to-film distances and nozzle and sample temperatures are given in Table S1.† The camera distances were calculated using diffraction patterns of benzene recorded immediately after each of the sample runs. The scattering intensities were measured using an Epson Expression 1680 Pro flatbed scanner and converted to mean optical densities using a method described elsewhere.[38] The data were then reduced and analysed using the ed@ed least-squares refinement program v2.4,[39] employing the scattering factors of Ross et al.[40] The weighting points for the off-diagonal weight matrix, correlation parameters and scale factors are shown in Table S1.†

The GED refinement procedure used here for $Si_{10}O_{15}H_{10}$ gives interatomic distances that we have termed $r_{e,MD}$, indicating that corrections of the form $r_a–r_e$ have been determined from MD simulations described above. The calculated amplitudes of vibration used as starting values in the refinement were also taken from MD simulations, and are termed u_{MD}.

Preparation of $Si_{10}O_{15}H_{10}$

The $Si_{10}O_{15}H_{10}$ was prepared using a published method[6] and was purified first by extracting the $Si_{10}O_{15}H_{10}$ and some of the $Si_8O_{12}H_8$ into hexane, followed by the removal of the solvent and then vacuum sublimation of $Si_8O_{12}H_8$ from the product mixture. The purity was checked by ^1H NMR spectroscopy.

Results and discussion

Computational studies

Table 1 contains the results of geometry optimisations performed using various basis sets and levels of theory. The atom-numbering scheme used is shown in Fig. 1. The most notable feature of the calculations is the variation in Si(2)–O(12)–Si(3) and Si(3)–O(28)–Si(9) angles. While the distances remain unchanged at the RHF level of theory, swapping the 3-21G(d) basis set for 6–31G(d) narrows these angles by 2.1 and 2.6°, respectively. Retaining the 6–31G(d) basis set and including electron correlation with MP2 causes each of the unique Si–O distances to lengthen by 2.1 pm. However, while the Si(3)–O(28)–Si(9) angle remains almost unchanged, the Si(2)–O(12)–Si(3) angle narrows by
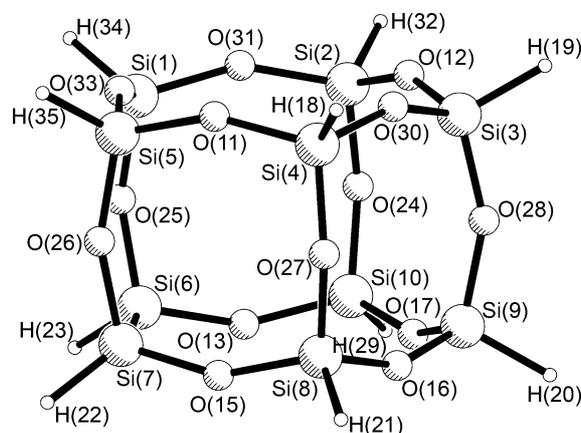

Fig. 1 Molecular structure of $Si_{10}O_{15}H_{10}$ including atom numbering.

Table 1 Calculated geometrical parameters for $Si_{10}O_{15}H_{10}$[a]

	rSi(2)–O(12)	rSi(3)–O(28)	rSi–H	∠Si(2)–O(12)–Si(3)	∠Si(3)–O(28)–Si(9)
RHF/3-21G(d)	162.1	162.4	145.3	157.5	155.4
RHF/6-31G(d)	162.1	162.4	145.4	155.4	152.8
MP2/6-31G(d)	164.2	164.5	146.5	153.2	152.9
MP2/6-311G(d)	163.4	163.9	146.0	155.0	152.3
MP2/6-311+G(d)	163.7	164.0	146.2	152.9	155.6
MP2/6-311++G(3df,3pd)	162.4	162.7	145.5	152.7	153.6
B3LYP/6-311++G(3df,3pd)	162.4	162.8	145.9	153.6	152.9
B3LYP/aug-cc-pVDZ	163.1	163.5	146.4	153.7	151.8
RHF//6-31G(d)/6-31G(d)[b]	162.5	162.9	145.9	155	152
LDA[c]	164	164	—	140.5	174.6
NLDA[d]	167	167	—	149.0	153.3
HF/VTZ(d,p)[e]	161.9	162.4	145.7	156.3	153.8
B3LYP/6-311G(d,p)[f]	163.7	164.2	146.2	155.9	152.0

[a] Distances are in pm, angles are in degrees. See Fig. 1 for atom numbering scheme. [b] A different version of the 6-31G(d) basis set was used for silicon than was used for oxygen and hydrogen; see ref. 10. [c] Local density approximation using the Vosko-Wilk-Nusair local exchange and correlation functional; see ref. 11. [d] Non-local density approximation using the gradient-corrected exchange functional of Becke with the Vosko–Wilk–Nusair correlation functional; see ref. 11. [e] See ref. 9. [f] See ref. 8.

a further 2.2°. Replacing 6–31G(d) with the larger 6–311G(d) basis set shortens the Si(2)–O(12) and Si(3)–O(28) distances by 0.8 and 0.6 pm, respectively. It also causes the Si(3)–O(28)–Si(9) angle to narrow by a modest 0.6°, whilst the Si(2)–O(12)–Si(3) angle widens by 1.8°. Adding diffuse functions to the heavy atoms lengthens the Si–O distances by no more than 0.3 pm, but narrows the Si(2)–O(12)–Si(3) angle by 2.1° and widens the Si(3)–O(28)–Si(9) angle by 3.3°. With diffuse functions on all atoms as well as additional polarisation functions [MP2/6-311++G(3df,3pd)], which gave the best results in our previous work on $Si_8O_{12}H_8$ and $Si_8O_{12}Me_8$,[20] there is another large change in the Si(3)–O(28)–Si(9) angle, while the Si(2)–O(12)–Si(3) angle is hardly affected. Using this level of theory and basis set also shortens the Si–O bonds by 1.3 pm. Further calculations at the B3LYP/6-311++G(3df,3pd) level demonstrate that the distances are as well defined as with MP2 theory, while the angles continue to change with no apparent pattern. At the B3LYP level using the correlation-consistent aug-cc-pVDZ basis set the Si–O bond lengths are slightly longer than those calculated using the best Pople-style basis sets. Cartesian coordinates corresponding to the structure calculated at the MP2/6-311++G(3df,3pd) level are given in Table S2.†

The large variations in the Si–O–Si angles are a reflection of the flexibility of these moieties, and although the fluctuations are large in structural terms, they are probably no greater than those of other structural parameters in terms of energy. This serves as a reminder that calculations of structure do not necessarily achieve the same level of accuracy for all distances or all angles, and that experimental data are of great importance for highly flexible systems.

A selection of calculated parameters taken from the literature for $Si_{10}O_{15}H_{10}$ is also given in Table 1. Pleasingly, parameters from the two calculations that follow similar theories to our own [RHF//6-31G(d)/6-31G(d)[10] and B3LYP/6-311G(d,p)[8]] give very similar results. Local density approximation (LDA) and non-local density approximation (NLDA) calculations have also been performed in the past.[11] Neither gives results for these parameters that are close to either the other calculated values or the experimental GED values. In particular the Si(3)–O(28)–Si(9) angle from the LDA calculation, 174.6°, is almost 20° wider than any other calculated

Table 2 Refined $r_{e,MD}$ parameters from the GED refinement for $Si_{10}O_{15}H_{10}$[a]

Parameter		$r_{e,MD}$	r_e[b]	Restraint
Independent				
p_1	rSi–H	145.7(7)	145.5	145.6(10)[c]
p_2	$r[2×Si(2)–O(12)/3 + Si(3)–O(28)/3]$	161.77(3)	162.5	—
p_3	$r[Si(2)–O(12) – Si(3)–O(28)]$	–0.6(4)	–0.3	–0.3(5)
p_4	∠Si(2)–O(12)–Si(3)	155.0(5)	152.7	—
p_5	∠Si(3)–O(28)–Si(9)	153.9(7)	153.6	—
p_6	∠X–A–O[d]	103.1(5)	102.7	102.7(5)
p_7	∠X–Si–H[d]	148.5(9)	147.9	147.9(10)
Dependent				
p_8	rSi(2)–O(12)	161.6(2)	162.4	—
p_9	rSi(3)–O(28)	162.2(3)	162.7	

[a] Distances are in pm, angles are in degrees. See Fig. 1 for atom numbering. The numbers in parentheses are estimated standard deviations of the last digits. [b] Theoretical results from MP2/6-311++G(3df,3pd) calculations. [c] This restraint was determined from the published IR stretch for this molecule (ref. 3) using the method outlined by McKean et al. (ref. 41). [d] X is the point at the centre of the pentagon formed by five Si atoms and A is the Si···Si midpoint for two adjacent Si atoms on the five-sided face.
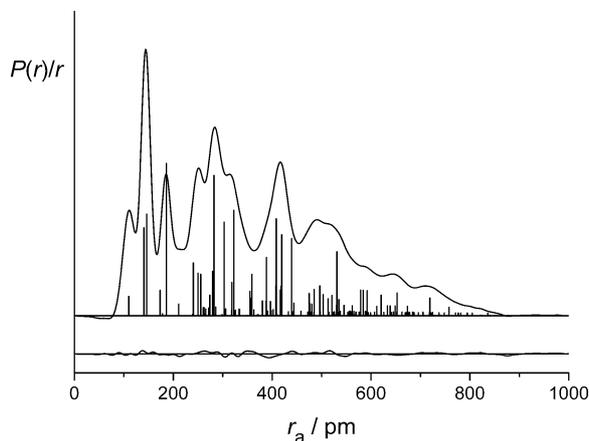
angle. The HF/VTZ(d,p) calculation,[9] on the other hand, seems to give very reasonable values, suggesting that quality of basis set and not of theory is important for this molecule.

GED refinement

A molecular model was written for $Si_{10}O_{15}H_{10}$ to allow the refinable geometrical parameters to be converted into Cartesian coordinates. The high symmetry of the molecule (D_{5h}) allowed the geometry to be described using only seven parameters (see Table 2), namely the Si–H distance, two Si–O distances described as a weighted average of the two and the difference between them, (p_{1-3}), the Si(2)–O(12)–Si(3) and Si(3)–O(28)–Si(9) angles (p_{4-5}), and a parameter ∠X–A–O (p_6), used to place the oxygen atoms with respect to the five-sided faces formed by the silicon atoms, with X the point at the centre of the pentagonal face and A lying

half way between a pair of silicon atoms on the edge nearest the oxygen atom. The final parameter defines the position of the H atom in the mirror plane (p_7). See Fig. 1 for a picture of the molecular structure complete with atom numbering.

For the refinement of the structure of $Si_{10}O_{15}H_{10}$ a flexible SARACEN restraint[42] was applied to the Si–H bond length using the solid-state IR stretch value and the method described by McKean et al.[41] A conservative uncertainty of 1 pm was employed. The X–A–O and X–Si–H angles were restrained to their calculated values [MP2/6-311++G(3df,3pd)] as they proved to be poorly defined. Amplitudes of vibration for distances under the same peak in the radial-distribution curve (RDC) were constrained by ratios fixed at the calculated values and only one amplitude for each group was refined. A full list of amplitudes of vibration, their constraints and the corresponding distances for each atom pair is given in Table S3.† A further flexible restraint was applied to u_1 [Si(1)–H(34)] using an uncertainty of 10% of its starting value. With these restraints in place all parameters and many significant RMS amplitudes of vibration were refined. The final R_G factor for the fit between the theoretical scattering (generated from the model) and the experimental data for $Si_{10}O_{15}H_{10}$ was 0.067 (R_D = 0.033). The final radial-distribution curve is shown in Fig. 2 and the corresponding molecular-intensity scattering curves are shown in Fig. S1.† Coordinates for the final structure are given in Table S4 and the least-squares correlation matrix is in Table S5.†

The use of molecular dynamics to give the distance correction terms and amplitudes of vibration for the analysis of the electron diffraction data was essential in this case. The atomic motions in this molecule, as in the related octasilsesquioxanes,[7] are complex, and not well represented by the commonly used methods involving a first-order approximation to curvilinear motion and quadratic or cubic force fields. The molecular dynamics method covers displacements of any complexity, and without limitation on the force field. However, the method we use at present does suffer from one significant restriction; although the forces are calculated quantum mechanically, the subsequent atomic motions depend on classical mechanics. This appears to give good distance corrections, but calculated amplitudes of vibration are somewhat small, particularly for atom pairs involving hydrogen. The amplitude for the Si–H bond was therefore replaced by a typical value. We have investigated the use of path-integral molecular dynamics (PIMD), which allows for quantum-mechanical tunnelling. Early indications are that it gives very accurate amplitudes of vibration, but the computational cost is great, and it is not yet appropriate to use the method for a molecule as large as $Si_{10}O_{15}H_{10}$.[29] However, the PIMD study did serve to show that classical MD does give good distance corrections, and that the combination of these corrections with amplitudes of vibration calculated by standard force-field methods is valid.

Comparison of structures

The structure of $Si_{10}O_{15}H_{10}$ in the gas phase is quite different from that in the crystal. The latter has been determined at 295 and 180 K, below which there is a change to a phase that has not yet been studied further. The present computational study, confirmed by experiment, shows unequivocally that the gas-phase molecules have D_{5h} symmetry, which of course cannot be retained in the crystal. The pentagonal prismatic structure includes two ten-membered rings, as well as five eight-membered rings. This is a pattern quite rare in zeolites.[43] In common with other silsesquioxanes, the $XSiO_3$ moieties are relatively rigid, but the flexibility of the Si–O–Si groups allows easy deformation of the cage.

Parameters for gas- and solid-phase molecules given in Table 3 show that there is little difference between the two types of Si–O distances in the gas phase, while there is a suggestion that in the crystal the bonds in the eight-membered rings are slightly longer than those in the large rings. There is a clear and consistent

Fig. 2 Experimental and difference (experimental minus theoretical) radial-distribution curves, $P(r)/r$, for $Si_{10}O_{15}H_{10}$. Before Fourier inversion the data were multiplied by $s \cdot \exp(-0.00002s^2)/(Z_{Si} - f_{Si})(Z_O - f_O)$.

Table 3 Geometrical parameters for $Si_{10}O_{15}R_{10}$ (R = H, Me)[a]

	R = H, gas		R = H, solid[b,c]		R = Me, solid[b,d]
	$r_{e,MD}$	r_e[e]	180 K	295 K	
10-membered ring					
rSi–O	161.6(2)	162.4	160.1(5)	159.6(6)	159.9(5)
∠Si–O–Si	155.0(5)	152.7	154.7(31)	154.9(22)	155.0(43)
8-membered ring					
rSi–O	162.2(3)	162.7	161.2(2)	160.8(4)	161.3(3)
∠Si–O–Si	153.9(7)	153.6	149.5(17)	149.3(13)	149.2(21)

[a] Distances are in pm, angles are in degrees. The numbers in parentheses are estimated standard deviations of the last digits. [b] Average values. [c] Ref. 7. [d] Ref. 44. [e] Theoretical results from MP2/6-311++G(3df,3pd) calculations.

difference in the Si–O–Si angles in all three crystal structures, with the average angles in the ten-membered rings wider than those in the eight-membered rings by 5 to 6°. However, there are considerable variations within each set, which accounts for the large standard deviations of the means given in the table; the esds of the individual angles are all around 0.2°. In contrast, the difference between the two kinds of Si–O–Si angles in the gas phase is only about 1°. Thus there is clear evidence for substantial distortion in the crystalline-phase structures that have been reported. The nature of this distortion has been subjected to principal component analysis,[7] revealing that almost all of it can be attributed to two doubly degenerate components. Both involve extension and compression of the two ten-membered rings, in one case with the rings deforming in phase with one another, and in the other out of phase. These correspond to the two lowest frequency vibration modes in our RHF/6-31G(d) frequency calculation. The eigenvectors are plotted in Fig. S2 and S3.†

The flexibility of the ten-membered rings in the gas-phase structure can be gauged by looking at the amplitudes of vibration from the GED refinement. For $Si(1)\cdots Si(3)$, the longer non-bonded silicon–silicon interaction across the ring, the amplitude of vibration is 22.1 pm. This is much larger than the amplitude of vibration for the shorter non-bonded $Si\cdots Si$ interaction $\{u[Si(1)\cdots Si(2)] = 9.0\ \text{pm}\}$. Even more striking is the amplitude of vibration for $Si(1)\cdots O(30)$, which at 47.8 pm is amongst the largest seen in these molecules. The flexibility of the cage seems to have more to do with the oxygen atoms than the silicon atoms.

The presence of large-amplitude low-frequency modes of vibration is also apparent from the MD simulations. During the simulations the cage undergoes significant distortions from ideal symmetry, with the ten-membered rings showing a great deal more flexibility than the eight-membered rings. In particular, the ten-membered rings can be seen to undergo the types of motions that the solid-state principal component analysis suggests are the root cause of the solid-state distortions from D_{5h} molecular symmetry. Such motions, which one could not expect to model through use of calculation of quadratic or cubic force fields, further justify our use of the MD method for determining the structure of $Si_{10}O_{15}H_{10}$.

It is clear that the large ten-membered rings in this molecule make it exceptionally flexible. This is shown also by surprisingly large anisotropic displacement parameters in the crystal structures of $Si_{10}O_{15}(OR)_{10}$ (R = SiMe$_3$ and SiMe$_2$H),[45] originally interpreted in term of disorder, but which we believe really reflect large vibrational motions.

One might expect to find even more flexibility in larger rings in higher silsesquioxanes, but in fact the structure of dodecahydridosilsesquioxane, $Si_{12}O_{18}H_{12}$, is not a hexagonal biprism, but has a structure with eight- and ten-membered rings.[46] Molecules with ten-membered rings are therefore likely to be the most easily distorted members of this large family of molecules, and the reduction of intramolecular distances as they distort is potentially useful. Trans-cage atomic-pair distributions are likely to show negative anharmonicity, and therefore may be associated with negative thermal expansion of the cage.

Given the similarity of the structural parameters in the rings of different sizes in gas-phase $Si_{10}O_{15}H_{10}$, one might expect those parameters to be close to those found in $Si_8O_{12}H_8$,[20] but that is not the case. The Si–O bond lengths are indeed similar, at 161.41(3) pm in $Si_8O_{12}H_8$ and 162.2(3) pm in $Si_{10}O_{15}H_{10}$, but the Si–O–Si angles are 147.9(2) and 153.9(7)°, respectively. This is probably a reflection of the fact that the larger ring allows the oxygen atoms to be displaced more above the plane of the five silicon atoms without reduction of the distance between them, and this in turn allows corresponding widening of the angles in the smaller rings. We are currently investigating structures of silsesquioxanes with a range of ring sizes, and expect that patterns in the structural parameters will emerge.

References

1 P. D. Lickiss and F. Rataboul, *Adv. Organomet. Chem.*, 2008, **57**, 1.
2 G. Li and C. U. Pittman, *Macromol. Containing Met. Met.-Like Elem.*, 2005, **4**, 79.
3 C. L. Frye and W. T. Collins, *J. Am. Chem. Soc.*, 1970, **92**, 5586.
4 S. Tang and R. Yang, *Jingxi Huagong*, 2006, **23**, 227.
5 P. A. Agaskar and W. G. Klemperer, *Inorg. Chim. Acta*, 1995, **229**, 355.
6 P. A. Agaskar, *Inorg. Chem.*, 1991, **30**, 2707.
7 H.-B. Bürgi, K. W. Törnroos, G. Calzaferri and H. Bürgy, *Inorg. Chem.*, 1993, **32**, 4914.
8 D. Hossain, C. U. Pittman, Jr., S. Saebo and F. Hagelberg, *J. Phys. Chem. C*, 2007, **111**, 6199.
9 B. Tejerina and M. S. Gordon, *J. Phys. Chem. B*, 2002, **106**, 11764.
10 C. W. Earley, *J. Phys. Chem.*, 1994, **98**, 8693.
11 K.-H. Xiang, R. Pandey, U. C. Pernisz and C. Freeman, *J. Phys. Chem. B*, 1998, **102**, 8704.
12 M. Bärtsch, P. Bornhauser, G. Calzaferri and R. Imhof, *Vib. Spectrosc.*, 1995, **8**, 305.
13 J. N. Greeley and M. M. Banaszak Holl, *Inorg. Chem.*, 1998, **37**, 6014.
14 M. Bärtsch, G. Calzaferri and C. Marcolli, *Res. Chem. Intermed.*, 1995, **21**, 577.
15 C. Marcolli, P. Laine, R. Bühler, G. Calzaferri and J. Tomkinson, *J. Phys. Chem. B*, 1997, **101**, 1171.
16 K. T. Nicholson, K. Z. Zhang, M. M. Banaszak Holl, F. R. McFeely and U. C. Pernisz, *Langmuir*, 2000, **16**, 8396.
17 K. Z. Zhang, L. M. Meeuwenberg, M. M. Banazak Holl and F. R. McFeely, *Jpn. J. Appl. Phys., Part 1*, 1997, **36**, 1622.
18 S. B. Desu, C. H. Peng, T. Shi and P. A. Agaskar, *J. Electrochem. Soc.*, 1992, **139**, 2682.
19 I. Rushkin, O. N. Dimov, S. Malik and B. B. De, US Patent 2008/0199805 A1.
20 D. A. Wann, R. J. Less, F. Rataboul, P. D. McCaffrey, A. M. Reilly, H. E. Robertson, P. D. Lickiss and D. W. H. Rankin, *Organometallics*, 2008, **27**, 4183.
21 M. J. Frisch, G. W. Trucks, H. B. Schlegel, G. E. Scuseria, M. A. Robb, J. R. Cheeseman, J. A. Montgomery, Jr., T. Vreven, K. N. Kudin, J. C. Burant, J. M. Millam, S. S. Iyengar, J. Tomasi, V. Barone, B. Mennucci, M. Cossi, G. Scalmani, N. Rega, G. A. Petersson, H. Nakatsuji, M. Hada, M. Ehara, K. Toyota, R. Fukuda, J. Hasegawa, M. Ishida, T. Nakajima, Y. Honda, O. Kitao, H. Nakai, M. Klene, X. Li, J. E. Knox, H. P. Hratchian, J. B. Cross, V. Bakken, C. Adamo, J. Jaramillo, R. Gomperts, R. E. Stratmann, O. Yazyev, A. J. Austin, R. Cammi, C. Pomelli, J. Ochterski, P. Y. Ayala, K. Morokuma, G. A. Voth, P. Salvador, J. J. Dannenberg, V. G. Zakrzewski, S. Dapprich, A. D. Daniels, M. C. Strain, O. Farkas, D. K. Malick, A. D. Rabuck, K. Raghavachari, J. B. Foresman, J. V. Ortiz, Q. Cui, A. G. Baboul, S. Clifford, J. Cioslowski, B. B. Stefanov, G. Liu, A. Liashenko, P. Piskorz, I. Komaromi, R. L. Martin, D. J. Fox, T. Keith, M. A. Al-Laham, C. Y. Peng, A. Nanayakkara, M. Challacombe, P. M. W. Gill, B. G. Johnson,

W. Chen, M. W. Wong, C. Gonzalez and J. A. Pople, *GAUSSIAN 03 (Revision C.01)*, Gaussian, Inc., Wallingford, CT, 2004.

22 National Service for Computational Chemistry Software (NSCCS), URL http://www.nsccs.ac.uk.

23 (*a*) J. S. Binkley, J. A. Pople and W. J. Hehre, *J. Am. Chem. Soc.*, 1980, **102**, 939; (*b*) M. S. Gordon, J. S. Binkley, J. A. Pople, W. J. Pietro and W. J. Hehre, *J. Am. Chem. Soc.*, 1982, **104**, 2797; (*c*) W. J. Pietro, M. M. Francl, W. J. Hehre, D. J. DeFrees, J. A. Pople and J. S. Binkley, *J. Am. Chem. Soc.*, 1982, **104**, 5039.

24 (*a*) W. J. Hehre, R. Ditchfield and J. A. Pople, J. A., *J. Chem. Phys.*, 1972, **56**, 2257; (*b*) P. C. Hariharan and J. A. Pople, *Theor. Chim. Acta*, 1973, **28**, 213; (*c*) M. S. Gordon, *Chem. Phys. Lett.*, 1980, **76**, 163.

25 (*a*) R. Krishnan, J. S. Binkley, R. Seeger and J. A. Pople, *J. Chem. Phys.*, 1980, **72**, 650; (*b*) A. D. McLean and G. S. Chandler, *J. Chem. Phys.*, 1980, **72**, 5639.

26 C. Møller and M. S. Plesset, *Phys. Rev.*, 1934, **46**, 618.

27 (*a*) A. D. Becke, *J. Chem. Phys.*, 1993, **98**, 5648; (*b*) C. Lee, W. Yang and R. G. Parr, *Phys. Rev. B*, 1992, **37**, 785; (*c*) B. Miehlich, A. Savin, H. Stoll and H. Preuss, *Chem. Phys. Lett.*, 1989, **157**, 200.

28 T. H. Dunning, Jr., *J. Chem. Phys.*, 1989, **90**, 1007; R. A. Kendall, T. H. Dunning, Jr. and R. J. Harrison, *J. Chem. Phys.*, 1992, **96**, 6769; D. E. Woon and T. H. Dunning, Jr., *J. Chem. Phys.*, 1993, **98**, 1358.

29 D. A. Wann, A. V. Zakharov, A. M. Reilly, P. D. McCaffrey and D. W. H. Rankin, *J. Phys. Chem. A*, in press.

30 CPMD, Version 3.11.1, IBM Corp. 1990–2006, MPI für Festkörperforschung, Stuttgart, 1997–2001.

31 G. J. Martyna and M. E. Tuckerman, *J. Chem. Phys.*, 1999, **110**, 2810.

32 J. P. Perdew, K. Burke and M. Ernzerhof, *Phys. Rev. Lett.*, 1996, **77**, 3865.

33 N. Troullier and J. L. Martins, *Phys. Rev. B*, 1991, **43**, 1993.

34 W. G. Hoover, *Phys. Rev. A*, 1985, **31**, 1695.

35 S. Nosé, *J. Chem. Phys.*, 1984, **81**, 511.

36 R. Car and M. Parrinello, *Phys. Rev. Lett.*, 1985, **55**, 2471.

37 C. M. Huntley, G. S. Laurenson and D. W. H. Rankin, *J. Chem. Soc., Dalton Trans.*, 1980, 954.

38 H. Fleischer, D. A. Wann, S. L. Hinchley, K. B. Borisenko, J. R. Lewis, R. J. Mawhorter, H. E. Robertson and D. W. H. Rankin, *Dalton Trans.*, 2005, 3221.

39 S. L. Hinchley, H. E. Robertson, K. B. Borisenko, A. R. Turner, B. F. Johnston, D. W. H. Rankin, M. Ahmadian, J. N. Jones and A. H. Cowley, *Dalton Trans.*, 2004, 2469.

40 A. W. Ross, M. Fink and R. Hilderbrandt, *International Tables for Crystallography*, ed. A. J. C. Wilson, Kluwer, Academic Publishers, Dordrecht, Netherlands, 1992, vol. C, p. 245.

41 D. C. McKean, I. Torto, J. E. Boggs and K. Fan, *J. Mol. Struct. (THEOCHEM)*, 1992, **260**, 27.

42 (*a*) A. J. Blake, P. T. Brain, H. McNab, J. Miller, C. A. Morrison, S. Parsons, D. W. H. Rankin, H. E. Robertson and B. A. Smart, *J. Phys. Chem.*, 1996, **100**, 12280; (*b*) P. T. Brain, C. A. Morrison, S. Parsons and D. W. H. Rankin, *J. Chem. Soc., Dalton Trans.*, 1996, 4589; (*c*) N. W. Mitzel and D. W. H. Rankin, *Dalton Trans.*, 2003, 3650.

43 (*a*) G. T. Kokotailo, S. L. Lawton, D. H. Olson and W. M. Meier, *Nature*, 1978, **272**, 437; (*b*) E. M. Flanigen, J. M. Bennett, R. W. Grose, J. P. Cohen, R. L. Patton, R. M. Kirchner and J. V. Smith, *Nature*, 1978, **271**, 512; (*c*) B. B. Schaack, W. Schrader and F. Schüth, *Angew. Chem.*, 2008, **120**, 9232.

44 I. A. Baidina, N. V. Podberezskaya, S. V. Borisov, V. I. Alekseev, T. N. Martynova and A. N. Kanev, *Zh. Strukt. Khim.*, 1980, **21**, 125.

45 N. Auner, B. Ziemer, B. Herrschaft, W. Ziche, P. John and J. Weis, *Eur. J. Inorg,. Chem.*, 1999, 1087.

46 K. W. Törnroos, H.-B. Bürgi, G. Calzaferri and H. Bürgy, *Acta Crystallogr., Sect. B: Struct. Sci.*, 1995, **51**, 155.